Available online at http://ijim.srbiau.ac.ir/
Int. J. Industrial Mathematics (ISSN 2008-5621)
Vol. 8, No. 4, 2016 Article ID IJIM-00585, 17 pages
Research Article

Effect of slip and variable thermal boundary conditions on hydromagnetic mixed convection flow and heat transfer from a non-linearly stretching surface

M. Abd El-Aziz *†‡

Received Date: 2014-09-07 Revised Date: 2015-11-13 Accepted Date: 2015-12-09

Abstract

The effect of partial slip and temperature dependent fluid properties on the MHD mixed convection flow from a heated, non-linearly stretching surface in the presence of radiation and non-uniform internal heat generation/absorption is investigated. The velocity of the stretching surface was assumed to vary according to power-law form. Thermal transport is analyzed for two types of non-isothermal boundary conditions, i.e. variable wall temperature (VWT) and variable surface heat flux (VHF) of the power-law form. The analysis accounts for both temperature dependent viscosity and temperature dependent thermal conductivity. The governing differential equations are transformed by introducing proper non-similarity variables and are solved numerically. The physical significance of the slip parameter, magnetic parameter, radiation parameter, viscosity-temperature parameter, thermal conductivity parameter and buoyancy force parameter on the flow and the thermal fields are shown through graphs and discussed in detail. The values of wall shear stress and the local Nusselt number are tabulated.

Keywords : Slip flow; Mixed convection; Heat source; Stretching surface; Magnetic field; Radiation.

1 Introduction

Owing to their numerous applications in industrial manufacturing process, the problem of heat transfer in the boundary layers of a continuously stretching surface with a given temperature or heat flux moving in an otherwise quiescent fluid medium has attracted the attention of researchers for the past three decades. Some of the application areas are hot rolling, paper production, metal spinning, drawing plastic films, glass blowing, continuous casting of metals and spinning of fibers. Since the pioneer study of Sakiadis [17] who developed a numerical solution for the boundary layer flow field of a stretched surface, many authors have attacked this problem to study the hydrodynamic and thermal boundary layers due to a moving surface [24, 47, 11, 23, 20, 26, 13, 28, 18, 34, 48]. Although various aspects of this class of boundary layer problems have been tackled, the buoyancy forces on the momentum balance in the conservation equations were neglected in the above-cited reports [17, 24, 47, 11, 23, 20, 26, 13, 28, 18, 34, 48].

In actual practice, the flow over a continuous material moving through a quiescent fluid is induced by the movement of the solid material and

*Corresponding author. m_abdelaziz999@yahoo.com
†King Khaled University, Faculty of Science, Mathematics Department, Abha 9004, Saudi Arabia.
‡Department of Mathematics, Faculty of Science, Helwan University, Cairo, Egypt P. O. Box 11795.

by thermal buoyancy. Therefore, these two mechanisms, surface motion and buoyancy force will determine the momentum and thermal transport processes. The thermal buoyancy force arising due to the heating of a continuously moving surface, under some circumstances, may alter significantly the flow and thermal fields and thereby the heat transfer behavior in the manufacturing process. The following papers have taken the effect of buoyancy force into consideration. Such papers are those of Lin et al. [36], Karwe and Jaluria [51], Chen [30], and Ali [45]. In several practical applications, there exist significant temperature differences between the surface and the ambient fluid. This necessitates the consideration of temperature-dependent heat sources or sinks which may exert strong influence on the heat transfer characteristics (Vajravelu and Nayfeh [21]).

The study of heat generation or absorption effects in moving fluids is important in view of several physical problems such fluids undergoing exothermic or endothermic chemical reactions (Vajravelu and Hadjinicalaou [12]). In addition, mixed convection with heat generation can be applied to combustion modeling (Westphal et. al. [15]). Although, exact modeling of internal heat generation or absorption is quite difficult, some simple mathematical models can express its average behavior for most physical situations. Heat generation or absorption has been assumed to be constant, space-dependent or temperature-dependent (see for instance, Crepeau and Clarksean [31], Abo-Eldahab and Abd El-Aziz [5, 6, 7], Abd El-Aziz and Salem [8] and Salem and Abd El-Aziz [9]). All of the above-mentioned studies are based on constant physical properties.

It is known that some physical properties such as viscosity and thermal conductivity are functions of temperature [41] and assuming constant properties is a good approximation as long as small differences in temperature are involved. A more accurate prediction for the flow and heat transfer characteristics can be achieved by considering the variation of the physical properties with temperature. When applied to practical heat transfer problems with large temperature differences between the surface and the ambient fluid, the constant property assumption could cause significant errors, since the transport properties of most fluids vary with temperature. Therefore, the temperature dependency of the fluid properties is of dominant importance in many cases of energy transfer [52]. Pop et al. [46], and Elbashbeshy and Bazid [27] have studied the effect of variable viscosity using the similarity solution with no buoyancy force. Ali [25] studied the effect of temperature dependent viscosity on mixed convection heat transfer along a vertical moving surface taking into account the effect of buoyancy force. Abd El-Aziz [19] studied the effect of Ohmic heating on MHD three-dimensional flow, heat and mass transfer of a viscous incompressible fluid having temperature dependent viscosity as well as thermal conductivity over a stretching surface taking into account the effect of buoyancy force. In the entire stretching sheet problems (both hydrodynamic and hydromagnetic) mentioned earlier, radiation effect has not been considered. The interaction of buoyancy with thermal radiation has increased greatly during the last decade due to its important in many practical applications. It is known that thermal radiation may be quiet significant at high operating temperatures in engineering processes, under many non-isothermal situations, and in situations where convective heat transfer coefficients are small. In polymer processing industry, if the entire system involving the polymer extrusion process is placed in a thermally controlled environment, then Thermal radiation effect might play an important role in controlling heat transfer process. The knowledge of radiation heat transfer in the system can perhaps lead to a desired product with a sought characteristic. Also, radiation effects on the convective flow are important in context of space technology and processes involving high temperature and very little is known about the effects of radiation on the boundary layer flow of radiating fluid past body. In view of this, Abd El-Aziz [37] has investigated the problem of thermal radiation effects on magnetohydrodynamic mixed convection flow of a micropolar fluid past a continuously moving semi-infinite plate for high temperature differences. Recently, Abd El-Aziz [38] studied the radiation effects on heat and fluid flow over an unsteady stretching surface.

Hydromagnetic flows and heat transfer characteristics of electrically conducting and heat generating/absorbing fluids have become more important in recent years because of many important

applications. For example, in many metallurgical processes which involve cooling of continuous strips or filaments, these elements are drawn through a quiescent fluid. During this process, these strips are sometimes stretched. The properties of the final product depend to a great extent on the rate of cooling. This rate of cooling has been proven to be controlled and, therefore, the quality of the final product by drawing such strips in an electrically conducting fluid subject to a magnetic field [1]. The use of magnetic fields has been also used in the process of purification of molten metals from non-metallic inclusions. Many works have been reported on flow and heat transfer of electrically conducting fluids over a stretched surface in the presence of magnetic field [2, 3, 4]. But all the above investigators restricted their analyses to flow and heat transfer with no-slip boundary condition. The no-slip assumption is not consistent with all physical characteristics i.e., in some practical flow situations it is essential to replace the no-slip boundary condition by the partial slip boundary condition. In the recent years, micro-scale fluid dynamics in the Micro- Electro-Mechanical Systems (MEMS) received much attention in research. Because of the micro-scale dimensions, the fluid flow behavior belongs to the slip flow regime is greatly differs from the traditional flow and the no slip condition at the solid-fluid interface is no longer applicable [42]. For the flow in the slip regime, the fluid motion still obeys the Navier-Stokes equations, but with slip velocity or temperature boundary conditions. A slip flow model more accurately describes the non-equilibrium region near the interface. A partial slip may occur on a stationary and moving boundary when the fluid is particulate such as emulsions, suspensions, foams, and polymer solutions. The partial slip condition was used in studies of a fluid flow past a permeable wall by Beavers and Joseph [44]. The slip flows under different flow configurations have been studied in recent years [35, 14, 10, 40]. Recently, Turkyilmazoglu [33] studied the unsteady mixed convective boundary layer flow and heat transfer over a porous stretching vertical surface in presence of slip.

Based on the above mentioned investigations and applications, the present work is to study the radiation effect on MHD mixed convection slip flow of an optically thick viscous fluid from a heated, continuously moving surface with non-uniform surface motion and variable thermal boundary conditions. In the analysis, power-law surface velocity variation was assumed for the continuously stretching sheet subject to two surface heating conditions: variable wall temperature (VWT) and variable surface heat flux (VHF) of the power law form. The variation of the viscosity and thermal conductivity with temperature in the presence non-uniform heat source/sink is considered. The governing differential equations are transformed into dimensionless forms using suitable nondimensional variables and then solved numerically. Results are obtained for the local Nusselt number and the local friction coefficient and presented for a wide range of various governing parameters to explore the basic characteristics of the flow and thermal transport processes. The results of these studies are of great importance, for example in the prediction of skin friction (or shear wall stress rate) as well as heat transfer rate over a stretching sheet which would find applications in technological and manufacturing industries such as polymer extrusion to obtain quality final product.

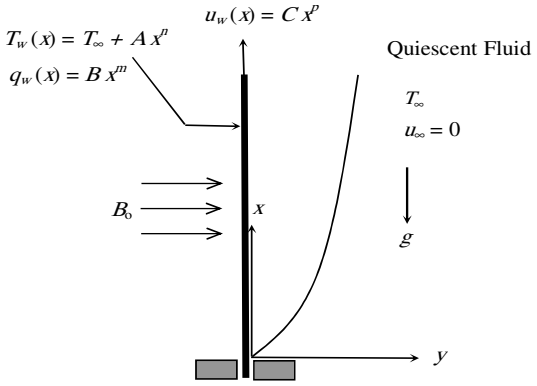

Figure 1: Physical model and coordinates.

2 Analysis

A steady laminar two-dimensional mixed heat convective flow of an optically thick electrically conducting viscous fluid along a heated continuously moving sheet is considered. The continuous flat sheet originates from a slot and is moving with a power-law velocity, $u_w(x) = Cx^p$ (where C is a constant of proportionality and p is a power index) in a vertical direction through a quiescent ambient fluid at temperature T_∞. The

Table 1: Comparison of the values of $Nu_x Re_x^{-1/2}$ for forced convection flow on a continuous iso-thermal sheet of uniform motion with $\lambda = M = A^* = B^* = \delta = 0, R \to \infty$ and $\theta_r \to \infty$

Pr	Tsou et al. [24]	Soundagekar and Murty [23]	Ali [18]	Present study
0.7	0.3492	0.3508	0.3476	0.3498
1.0	0.4438	–	0.4416	0.4438
10	1.6804	1.6808	1.6713	1.6803

Table 2: Comparison of the values of $\theta'(\xi, 0)$ for various values of Pr with p=1, $\lambda = M = A^* = B^* = n = \delta = 0, R \to \infty$ and $\theta_r \to \infty$

Pr	Gupta and Gupta [28]	Grubka and Bubba [11]	Ali [18]	Present study
0.7	–	–	-0.45255	-0.45445
1.0	-0.5820	l -0.5820	-0.59988	-0.58201
10	–	-2.3080	-2.29589	-2.30801

Table 3: Results of $Nu_x Re_x^{-1/2}$ for mixed convection flow on a continuously moving surface at $p = \xi = n = \delta = 0, \theta_r \to \infty$ (UWT csae), $p = \zeta = m = \varepsilon = 0, \phi_r \to \infty$ (UHF case) with $\lambda = M = A^* = B^* = 0$ and $R \to \infty$

	Pr =0.7		Pr =7.0	
	Moutsoglou and Chen [16]	Present study	Moutsoglou and Chen [16]	Present study
ξ (UWT case)				
0	0.34924	0.34933	1.38703	1.38696
1	0.45505	0.45423	1.43712	1.43693
3	0.53681	0.53659	1.51864	1.51810
5	0.59086	0.59075	1.58510	1.58456
ζ (UHT case)				
0	0.60154	0.60169	2.22826	2.22816
1	0.67261	0.67295	2.23934	2.23870
3	0.74626	0.74651	2.25943	2.25899
5	-	0.79421	2.27827	2.27768

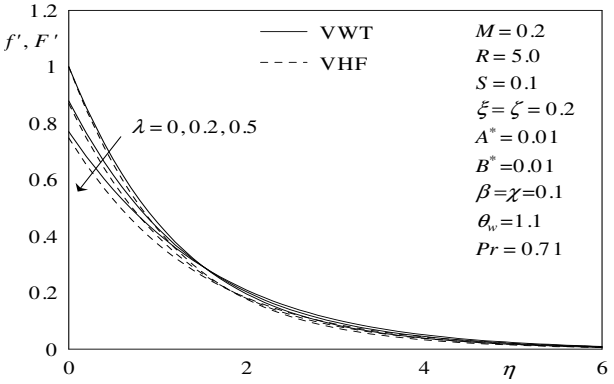

Figure 2: Velocity profiles for various values of λ.

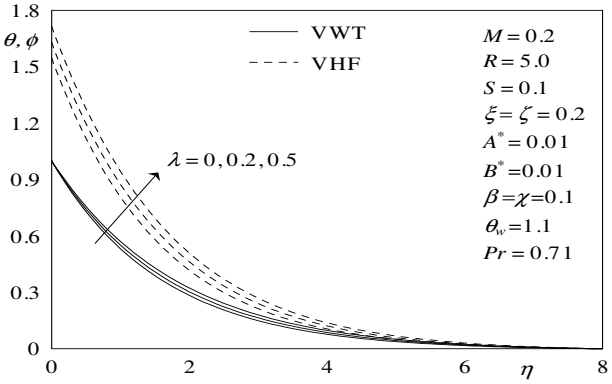

Figure 3: Temperature profiles for various values of λ.

non-linearly stretching sheet is assumed to be either subject to a power-law wall temperature, $T_w(x) - T_\infty = Ax^n$, or a power-law surface heat flux, $q_w(x) = Bx^m$. Here $T_w(x)$ and $q_w(x)$ are, respectively, temperature and heat flux at the wall, T_∞ is the temperature at large distance from the surface. A and B are dimensional constants, and m and n are exponents. The positive x coordinate is measured along the direction of motion with the slot as the origin and the positive

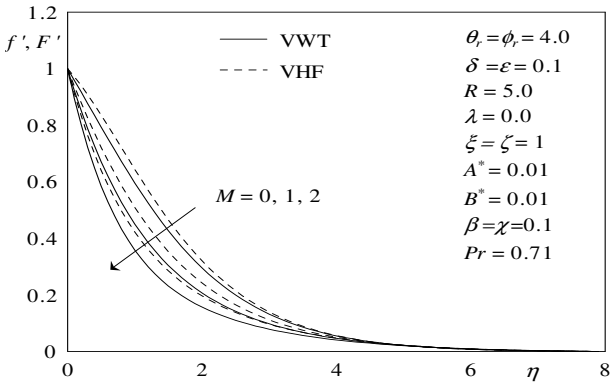

Figure 4: Velocity profiles for various values of M.

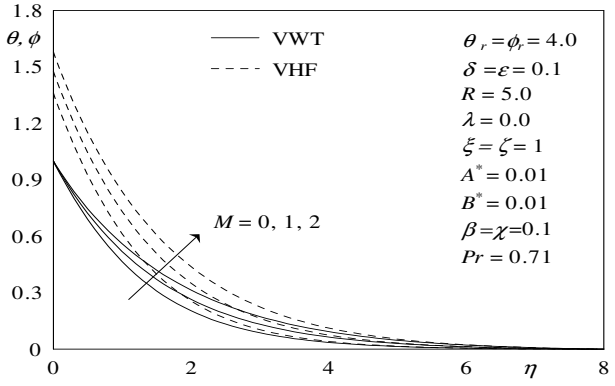

Figure 5: Temperature profiles for various values of M.

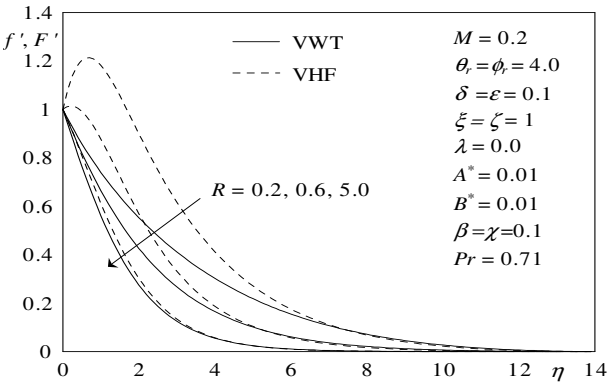

Figure 6: Velocity profiles for various values of R.

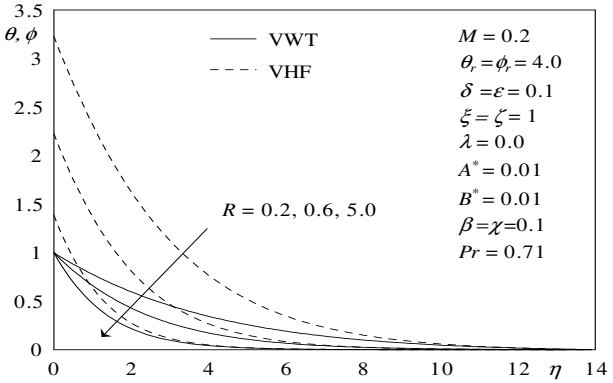

Figure 7: Temperature profiles for various values R

y coordinate is measured normal to the sheet in the outward direction toward the fluid. A magnetic field of strength B_0 is applied normal to the sheet in the y-direction (see Fig. 1). The magnetic Reynolds number is taken to be small enough so that the induced magnetic field can be neglected. The viscosity μ and thermal conductivity k of the fluid are assumed to be functions of temperature. The fluid is assumed to be Newtonian, electrically conducting, heat generating/absorbing. In addition, there is no applied electric field and the Hall effect, Joule heating and viscous dissipation are all neglected in this work. With the usual boundary layer and Boussnesq approximations the problem is governed by the following equations:

$$\frac{\partial u}{\partial x}+\frac{\partial v}{\partial y}=0 \tag{2.1}$$

$$u\frac{\partial u}{\partial x}+v\frac{\partial u}{\partial y}=\frac{1}{\rho}\frac{\partial \mu}{\partial T}\frac{\partial T}{\partial y}\frac{\partial u}{\partial y}+\frac{\mu}{\rho}\frac{\partial^2 u}{\partial y^2} \pm g\beta_0\left(T-T_\infty\right)-\frac{\sigma_0 B_0^2}{\rho}u \tag{2.2}$$

$$\rho c_p\left(u\frac{\partial T}{\partial x}+v\frac{\partial T}{\partial y}\right) = \frac{\partial k}{\partial T}\left(\frac{\partial T}{\partial y}\right)^2 +q'''-\frac{\partial q_r}{\partial y} \tag{2.3}$$

In the above equations, u and v denote the velocity components in the x and y directions, T is the temperature, k is the thermal conductivity, ρ is the fluid density, μ is the fluid dynamic viscosity, σ_0 is the electrical conductivity, c_p is the specific heat at constant pressure, β_0 is the volumetric coefficient of thermal expansion, q''' is the rate of internal heat generation (>0) or absorption (<0) coefficient, g is the acceleration due to gravity, B_0 is the magnetic induction and q_r is the local radiative heat flux.
The internal heat generation/absorption term q''' is modeled according to the following equations:

$$q''' = \frac{k_\infty u_w\left(x\right)}{\nu_\infty x}\left[A^* Q\left(x\right)\exp\left(-y\sqrt{\frac{u_w}{\nu_\infty x}}\right)\right] +\frac{k_\infty u_w\left(x\right)}{\nu_\infty x}\left[B^*\left(T-T_\infty\right)\right], \tag{2.4}$$

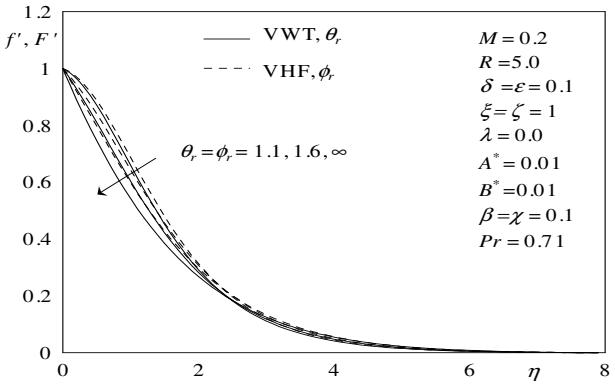

Figure 8: Velocity profiles for various values of θ_r and ϕ_r.

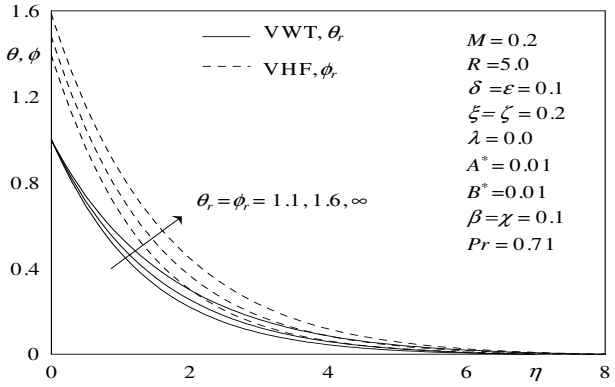

Figure 9: Temperature profiles for various values of θ_r and ϕ_r.

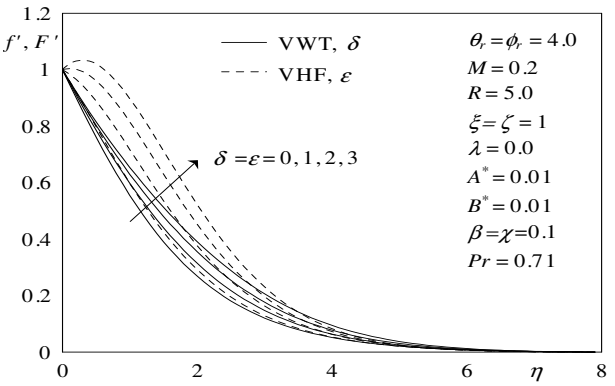

Figure 10: Velocity profiles for various values of δ and ε.

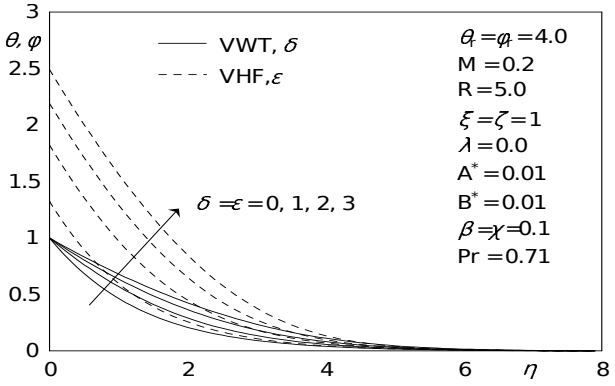

Figure 11: Temperature profiles for various values of δ and ε.

where

$$Q(x) = \begin{cases} (T_w - T_\infty) & \text{for VWT case} \\ \frac{q_w(x)}{k_\infty}\sqrt{\frac{\nu_\infty x}{u_w(x)}} & \text{for VWT case} \end{cases} \tag{2.5}$$

Where A^* and B^* are coefficients of space-dependent and temperature-dependent internal heat generation/absorption, respectively. In Eq. (2.4), the first term represents the dependence of the internal heat generation or absorption on the space coordinates while the latter term represents its dependence on the temperature. Note that when both $A^* > 0$ and $B^* > 0$, this case corresponds to internal heat generation while for both $A^* < 0$ and $B^* < 0$, the case corresponds to internal heat absorption. With the increase of temperature, the fluid viscosity in the momentum boundary layer decreases which in turn affects the heat transfer rate at the wall. Thus in order to predict the flow and heat transfer rates accurately, it is necessary to take into account the temperature dependence of the fluid viscosity. Ling and Dybbs [29] suggest a temperature dependent viscosity of the form:

$$\frac{1}{\mu} = \frac{1}{\mu_\infty}\left(1 + \gamma\left(T - T_\infty\right)\right) \tag{2.6}$$

where μ_∞ is the ambient fluid dynamic viscosity and γ is a thermal property of the fluid. Eq. (4) can be rewritten as:

$$\frac{1}{\mu} = a\left(T - T_r\right) \tag{2.7}$$

where $a = \gamma/\mu_\infty$and $T_r = T_\infty - 1/\gamma$ are constants and their values depend on the reference state and the thermal property of the fluid. In general, $a > 0$for liquids and $a < 0$ for gases.

The most common working fluids found in engineering applications are air and water. To further demonstrate the appropriateness of Eq. (2.4), correlations between viscosity and temperature for air and water are given below [50]

For air,

$$\frac{1}{\mu} = -132.2\left(T - 742.6\right), \tag{2.8}$$

based on $T_\infty = 293K$ (20^oC).

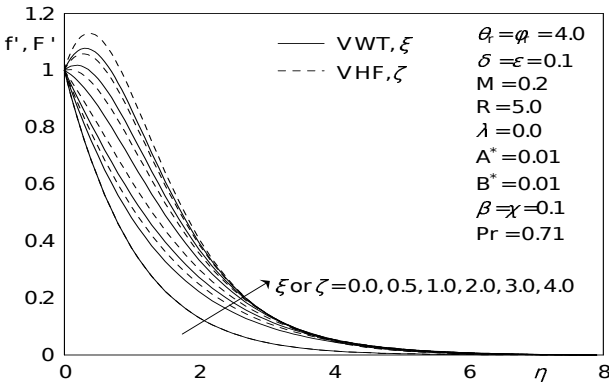

Figure 12: Velocity profiles for various values of ξ and ζ.

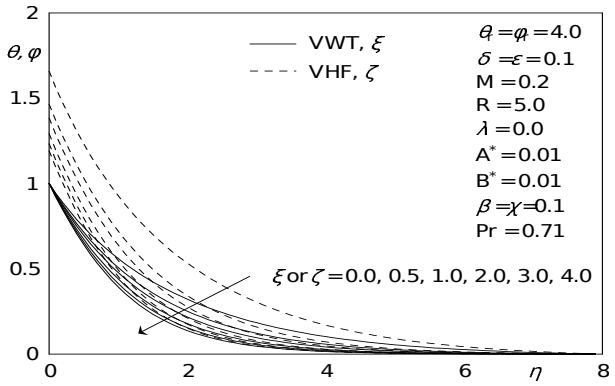

Figure 13: Temperature profiles for various values of ξ and ζ.

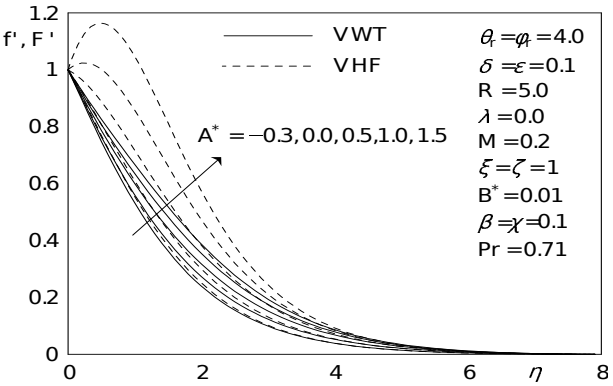

Figure 14: Velocity profiles for various values of A^*.

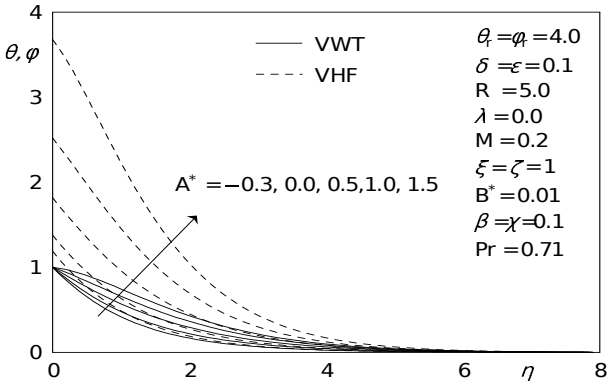

Figure 15: Temperature profiles for various values of A^*.

For water,

$$\frac{1}{\mu} = 29.83\,(T - 258.6) \tag{2.9}$$

based on $T_\infty = 288K$ (15^oC).

Savvas et al. [39] observed that for liquid metals, the thermal conductivity varies linearly with temperature in the range $0 - 400^o$F. We follow Savvas et al. [39] and assume the thermal conductivity of the fluid to be a linear function of the temperature. The specific model used is (see Chiam [16])

$$k = k_\infty\,(1 + b\,(T - T_\infty)) \tag{2.10}$$

Where b is a constant depending on the nature of the fluid and k_∞ is the ambient fluid thermal conductivity. In general, $b > 0$ for fluids such as water and air, while $b < 0$ for fluids such as lubricating oils.

By using the Rosseland approximation [49] we have:

$$q_r = -\frac{4\sigma}{3k_1}\frac{\partial T^4}{\partial y}, \tag{2.11}$$

where σ is the Stefan-Boltzmann constant and k_1 is the mean absorption coefficient.

The boundary conditions suggested by the physics of the problem are:

$$\begin{aligned} &u_w = u(x) + L\left(\frac{\partial u}{\partial y}\right), \quad v = 0, \\ &T_w\,(x) = T_\infty + Ax^n \quad \text{or} \\ &-k_\infty\left(\frac{\partial T}{\partial y}\right) = q_w\,(x) = Bx^m \quad \text{at} \quad y = 0, \\ &u \to 0, \quad T \to T_\infty \qquad \text{at} \quad y \to \infty \end{aligned} \tag{2.12}$$

where L is the slip length.

Case (I): Variable Wall Temperature (VWT), $T_w\,(x) - T_\infty = Ax^n$

We introduce the dimensionless variables:

$$\begin{aligned} &\eta = (y/x)Re_x^{1/2}, \quad \xi = Gr_x/Re_x^2, \\ &f(\xi,\eta) = \psi\,(x,y)\,/\left(\nu_\infty Re_x^{1/2}\right), \\ &\theta(\xi,\eta) = (T - T_\infty)/(T_w\,(x) - T_\infty) \end{aligned} \tag{2.13}$$

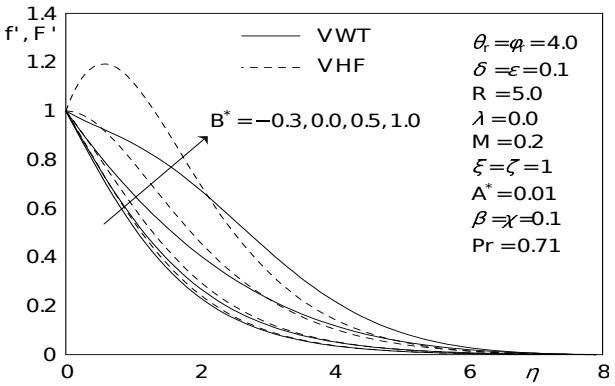

Figure 16: Velocity profiles for various values of B^*.

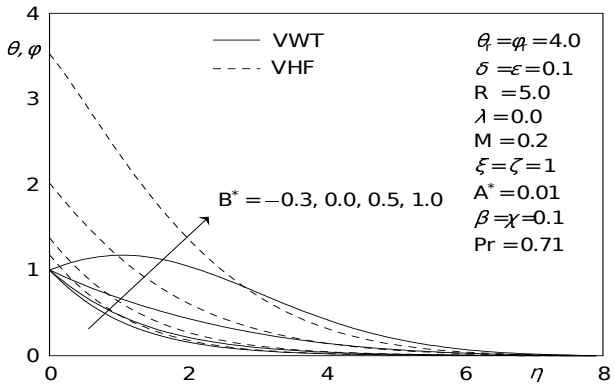

Figure 17: Temperature profiles for various values of B^*.

Where $Re_x = u_w(x)\,x/\nu_\infty$ is the local Reynolds number, $Gr_x = g\beta_0(T_w(x) - T_\infty)x^3/\nu_\infty^2$ is the local Grashof number and $f(\xi,\eta)$ is the stream function satisfying the continuity equation with $u = \partial\psi/\partial y$ and $v = -\partial\psi/\partial x$. Equations (2.2) and (2.3) under the transformation (2.13) reduce to:

$$\frac{\theta_r}{\theta_r-\theta}f''' + \frac{\theta_r}{(\theta_r-\theta)^2}f''\theta'$$

$$+\frac{1}{2}(p+1)\,ff'' - pf'^2 \pm \xi\theta - Mf' =$$

$$(n-2p+1)\,\xi\left(f'\frac{\partial f'}{\partial\xi} - f''\frac{\partial f}{\partial\xi}\right) \qquad (2.14)$$

$$(1+\delta\theta)\,\theta'' + \delta\theta'^2 + \frac{1}{2}(p+1)\,Pr_\infty f\theta'$$

$$-n\Pr_\infty f'\theta + \frac{4}{3R}\frac{\partial}{\partial\eta}\left[(1+\beta\theta)^3\,\theta'\right]$$

$$+A^*e^{-\eta} + B^*\theta$$

$$= Pr_\infty(n-2p+1)\,\xi\left(f'\frac{\partial\theta}{\partial\xi} - \theta'\frac{\partial f}{\partial\xi}\right) \qquad (2.15)$$

The primes indicate differentiation with respect to η, $M = \sigma_0 B_0^2 x/(\rho u_w)$ is the magnetic parameter, $\theta_r = (T_r - T_\infty)/(T_w - T_\infty)$ is the variable viscosity parameter for the VWT case, $\delta = b\,(T_w - T_\infty)$ is the thermal conductivity parameter, $R = k_\infty K_R/\left(4\sigma T_\infty^3\right)$ is the radiation parameter, $\beta = \Delta T/T_\infty$ is the temperature ratio parameter with $\Delta T = T_w - T_\infty$, $\Pr_\infty = \nu_\infty/\alpha$ is the ambient Prandtl number and $\alpha = k_\infty/\rho c_p$ is the thermal conductivity of the fluid. It is worth mentioning here that the range of variations [43] of δ for air is $0 \le \delta \le 6$, and for water is $0 \le \delta \le 0.12$, and for lubrication is $-0.1 \le \delta \le 0$. The transformed boundary conditions are given by:

$$f'(\xi,0) = 1 + \lambda f''(\xi,0),$$

$$f(\xi,0) = 0, \quad \theta(\xi,0) = 1$$

$$f'(\xi,\infty) = 0, \quad \theta(\xi,\infty) = 0 \qquad (2.16)$$

where $\lambda = L\sqrt{\frac{u_w}{x\nu_\infty}}$ is the slip parameter.

The physical quantities of interest are the local Nusselt number $Nu_x = hx/k_\infty$, where $h = q_w(x)/(T_w(x) - T_\infty)$ is the local heat transfer coefficient, $q_w(x) = -k\,(\partial T/\partial y)_{y=0}$ is the local surface heat flux, and $C_{fx} = 2\tau_{wx}/\left(\rho u_w^2\right)$ the local friction coefficient , with $\tau_{wx} = \mu\,(\partial u/\partial y)_{y=0}$denoting the local wall shear stress.

In terms of the transformation variables, theses quantities can be written as:

$$C_{fx}Re_x^{1/2} = \frac{2\theta_r}{\theta_r - 1}f''(\xi,0), \qquad (2.17)$$

$$Nu_xRe_x^{-1/2} = -(1+\delta)^{-1/2}\theta'(\xi,0) \qquad (2.18)$$

Case (II): Variable Heat Flux (VHF), $q_w(x) = Bx^m$

For this case, the following non-similarity variables are invoked:

$$\eta = (y/x)Re_x^{1/2}, \quad \xi = Gr_x/Re_x^{5/2},$$

$$F(\zeta,\eta) = \psi(x,y)/\left(\nu_\infty Re_x^{1/2}\right),$$

$$\phi(\zeta,\eta) = (T - T_\infty)Re_x^{1/2}/(xq_w(x)/k_\infty) \qquad (2.19)$$

where $Gr_x = g\beta_0 q_w(x)x^4/k_\infty\nu_\infty^2$ is the modified local Grashof number for the VHF case. In terms

of these variables the governing, Eqs. (2.2) and (2.3) are transformed into:

$$\frac{\phi_r}{\phi_r-\phi}f''' + \frac{\phi_r}{(\phi_r-\phi)^2}F''\phi' + \frac{1}{2}(p+1)FF'' - pF'^2 \pm \zeta\phi - MF' = \frac{1}{2}(2m-5p+3)\zeta\left(F'\frac{\partial F'}{\partial\zeta} - F'''\frac{\partial F}{\partial\zeta}\right) \quad (2.20)$$

$$(1+\varepsilon\phi)\phi'' + \varepsilon\phi'^2 + \frac{1}{2}(p+1)Pr_\infty F\phi' - \frac{1}{2}(2m-p+1)Pr_\infty F'\phi + \frac{4}{3R}\frac{\partial}{\partial\eta}\left[(1+\chi\phi)^3\phi'\right] + A^*e^{-\eta} + B^*\phi = \frac{1}{2}Pr_\infty(2m-5p+3)\zeta\left(F'\frac{\partial\phi}{\partial\zeta} - \phi'\frac{\partial F}{\partial\zeta}\right) \quad (2.21)$$

In the above equations $\phi_r = (T_r - T_\infty)/\left[(q_w(x)/k_\infty)\sqrt{x\nu_\infty/u_w(x)}\right]$, $\varepsilon = b\left((q_w(x)/k_\infty)\sqrt{x\nu_\infty/u_w(x)}\right)$ and $\chi = (q_w(x)/k_\infty)\sqrt{x\nu_\infty/u_w(x)}/T_\infty$are, respectively, the variable viscosity parameter, the thermal conductivity parameter and the temperature ratio parameter for the VHF case.

The transformed boundary conditions for the VHF case are given by:

$$\begin{aligned} &F'(\zeta,0) = 1+\lambda F''(\zeta,0),\\ &F(\zeta,0)=0,\quad \phi'(\zeta,0)=-1\\ &F'(\zeta,\infty)=0,\quad \phi(\zeta,\infty)=0 \end{aligned} \quad (2.22)$$

The local skin friction coefficients C_{fx} is defined as:

$$C_{fx}Re_x^{1/2} = \frac{2\phi_r}{\phi_r-\phi(\zeta,0)}F'(\zeta,0), \quad (2.23)$$

The local Nusselt number for this case is given by

$$Nu_xRe_x^{-1/2} = 1/\phi(\zeta,0) \quad (2.24)$$

3 Results and discussion

The transformed systems of Eqs. (2.14) - (2.15) for the VWT case and Eqs. (2.20)-(2.21) for the VHF case are approximated by a system of non-linear ordinary differential equations replacing the derivatives with respect to ξ (VWT case) and ζ (VHF case) by two-point backward finite difference with step size 0.01. These equations are integrated by fifth order Runge-Kutta-Fehlberg scheme with a modified version of the Newton-Raphson shooting method. Numerical computations are carried out for Pr = 0.71 (air), $p = n = m = 0.5$ and varies values of slip parameter λ, magnetic parameter M, the variable viscosity parameters (θ_r for the VWT case and ϕ_r for the VHF case), the thermal conductivity parameters (δ for the VWT case and ε for the VHF case), the buoyancy force parameters (ξ for the VWT case and ζ for the VHF case), the coefficients of space-dependent and temperature-dependent internal heat generation/absorption A^* and B^*, respectively and the radiation parameter R. The more general formulations presented in this study can be readily simplified to various special cases considered in previous works. To verify the validity and accuracy of the present analysis, results for the local Nusselt number $Nu_xRe_x^{-1/2}$ were compared to those reported by Tsou et al. [24], Soundagekar and Murty [23] and Ali [18] for no slip ($\lambda = 0$) forced convection flow on a continuous iso-thermal sheet ($n = 0$) with uniform motion ($p = 0$) (see Table 1). Also, Table 2 shows a comparison of the present results for the temperature gradient $-\theta'(0)$ with those reported by Gupta and Gupta [28], Grubka and Bobba [11] and Ali [18] for $\lambda = 0$ (no slip flow), $p = 1$(linearly stretching surface), $n = 0$ (iso-thermal sheet) and various values of Prandtl number Pr in the absence of magnetic field ($M = 0$), heat source/sink ($A^* = B^* = 0$), radiation ($R \to \infty$), viscosity and thermal conductivity temperature variations. Finally, Table 3 illustrates the comparison of $Nu_xRe_x^{-1/2}$values with those of Moutsoglou and Chen [32] for the case of no slip mixed convection flow past a stretching sheet moving with a constant speed ($p = 0$) for the UWT ($n = \delta = 0$, $\theta_r \to \infty$) and UHF ($m = \varepsilon = 0$, $\phi_r \to \infty$) cases with $M = A^* = B^* = 0$ and $R \to \infty$. In all cases, the results are found to be in good agreement. The numerical values of the dimensionless wall shear stress and the local Nusselt number in the VWT and VHF cases are listed in Tables 4 and 5, respectively. The results of the numerical computations are displayed in Figs. 2-17 for both

Table 4: $f''(\xi,0)$ and $Nu_x Re_x^{-1/2}$ for the VWT case for various values of $\lambda, M, R, \theta_r, \delta, \xi, A^*$ and B^* with p=n=0

λ	M	R	θ_r	δ	ξ	A^*	B^*	$f''(\xi,0)$	$Nu_x Re_x^{-1/2}$
0.0	0.2	5.0	4.0	0.1	0.1	0.01	0.01	-0.487532	0.771029
0.2	0.2	5.0	4.0	0.1	0.1	0.01	0.01	-0.380960	0.749960
0.5	0.2	5.0	4.0	0.1	0.1	0.01	0.01	-0.288421	0.730782
0.0	0.0							-0.400653	0.787437
0.0	1.0							-0.790634	0.713658
0.0	2.0							-1.100258	0.656801
		0.2						-0.312555	0.272724
		0.8						-0.404522	0.488892
		3.0						-0.471637	0.708453
			1.1					-0.104121	0.817762
			1.6					-0.323349	0.791674
			$\to\infty$					-0.559067	0.761877
				0.0				-0.493041	0.735549
				1.0				-0.447251	1.023804
				2.0				-0.415343	1.233174
				3.0				-0.391397	1.406281
					0.0			-0.920630	0.663835
					1.0			-0.487532	0.771029
					3.0			0.209674	0.867742
						-0.7		-0.559734	1.105624
						-0.3		-0.516566	0.915425
						0.0		-0.487532	0.771028
						0.5		-0.445937	0.546348
						1.5		-0.370609	0.097036
							-0.7	-0.5492405	1.091075
							-0.3	-0.5204291	0.925883
							0.0	-0.4888202	0.776563
							0.5	-0.3882637	0.413587
							1.5	0.2191793	-1.854221

VWT (solid lines) and VHF (dotted lines) cases for distribution of the velocity and temperature fields. This is done in this way so as to minimize the number of figures needed for the parametric study of the physical parameters involved in the problem. Figs. 2 and 3 are the graphical representation of the velocity $f'(\xi,\eta)$ and temperature $\theta(\xi,\eta)$ profiles in the VWT case for different values of the velocity slip parameter λ. Fig. 2 shows that the fluid velocity profiles decreases greatly near the plate where $0 < \eta_0 \leq 1.6$ but the opposite trend is true for $\eta \geq \eta_0$ as the slip parameter λ is increased. Increasing the value of λ will decrease the flow velocity because the pulling of the stretching sheet can be only partly transmitted to the fluid under the slip condition. On the other hand, a general decrease in temperature profile is observed with maximum at the plate surface and minimum far away from the plate. The magnitude of the temperature profiles increase slightly with an increase in the slip parameter λ. Analysis of Table 4 shows that the local skin-friction coefficient in terms of $f''(\xi,0)$ was found to increase while the local Nusselt number $Nu_x Re_x^{-1/2}$decreases as the slip parameter λ increases.

Control of boundary layer flow is of practical significance. Several methods have been developed for the purpose of artificially controlling the behavior of the boundary layer. The application of magnetohydrodynamic (MHD) principle is another method for affecting the flow field in the

Table 5: $F''(\zeta,0)$ and $Nu_x Re_x^{-1/2}$ for the VHT case for various values of λ, M, R, $\phi_r, \varepsilon, \xi, A^*$ and B^*

λ	M	R	ϕ_r	δ		A^*	B^*	$f''(\xi,0)$	$Nu_x Re_x^{-1/2}$
0.0	0.2	5.0	4.0	0.1	0.1	0.01	0.01	-0.343248	0.722663
0.2	0.2	5.0	4.0	0.1	0.1	0.01	0.01	-0.260441	0.711324
0.5	0.2	5.0	4.0	0.1	0.1	0.01	0.01	-0.191633	0.701754
0.0	0.0							-0.264109	0.735548
0.0	1.0							-0.620869	0.677862
0.0	2.0							-0.907407	0.633545
		0.2						0.720479	0.309708
		0.8						0.033548	0.491147
		3.0						-0.282678	0.671011
			1.1					-0.083443	0.752837
			1.6					-0.244070	0.735288
			$\to\infty$					-0.377108	0.717496
				0.0				-0.371949	0.754638
				1.0				-0.118668	0.548759
				2.0				0.080274	0.456294
				3.0				0.245011	0.401569
					0.0			-0.920630	0.603487
					1.0			-0.593106	0.683021
					3.0			0.431366	0.810745
						-0.7		-0.561338	1.004937
						-0.3		-0.449072	0.841370
						0.0		-0.347001	0.726381
						0.5		-0.122068	0.550258
						1.5		0.722544	0.271930
							-0.7	-0.546534	1.091075
							-0.3	-0.5204291	0.925883
							0.0	-0.4888202	0.776563
							0.5	-0.3882637	0.413587
							1.5	0.2191793	1.854221

desired direction by altering the structure of the boundary layer. Fig. 4 shows the velocity profile in the VWT case for various magnetic parameter M $(=0,1,2)$. The velocity curves show that the rate of transport is considerably reduced with the increase of M. It clearly indicates that the transverse magnetic field opposes the transport phenomena. This is due to the fact that variation of the magnetic parameter leads to the variation of the Lorentz force due to magnetic field and the Lorentz force produces more resistance to transport phenomena. In all cases the velocity vanishes at some large distance from the sheet. Fig. 5 exhibits the temperature profiles in the VWT case for the same set of values of the magnetic parameter M. In each case, temperature is found to decrease with the increase of η until it vanishes at $\eta \approx 8$. But the temperature is found to increase for any non-zero fixed value of η with the increase of M. Also, the effects on the flow and thermal fields become less so as the strength of the magnetic field increases. Table 4 shows that, a distinct fall in the wall shear stress accompanies a rise in M from 0 through 2. Thus, physically this amounts to a reduction in the drag as indicated by Gorla et al. [22]. Also, the local Nusselt number $Nu_x Re_x^{-1/2}$ is decreased with increasing the values of the magnetic parameter M.

The results incorporating the effects of radiation parameter R on the velocity and temperature profiles for the VWT case are presented in Figs. 6 and 7 respectively. We observe from these figures that the velocity $f'(\xi,\eta)$ and the temperature $\theta(\xi,\eta)$ decrease largely in the boundary layer flow region as the radiation parameter R

increases. This result can be explained by the fact that the increase of the radiation parameter R implies the release of heat energy from the flow region by mean of radiation, which in turn decreases the temperature and velocity of the fluid. Also, the figures show that the larger the R, the thinner the momentum and thermal boundary layer thickness at fixed values of η. Table 4 shows that, as R increases, the wall shear stress $f''(\xi,0)$ decreases while the local Nusselt number $Nu_x Re_x^{-1/2}$ is greatly increased. Effect of the viscosity-temperature parameter θ_r on the velocity and temperature profiles in the boundary layer for the VWT case is shown in Figs. 8 and 9, respectively. From Fig. 9, it is noticed that the effect of viscosity-temperature parameter is to increase the temperature profile. This is due to the fact that the increase of the fluid viscosity parameter θ_r makes an increase in the thermal boundary layer thickness, which results in an increase in the temperature profile $\theta(\xi,\eta)$. On the other hand, increases in the values of θ_r have an opposite effect on the velocity profiles $f'(\xi,\eta)$, i. e. it causes $f'(\xi,\eta)$ to decrease. However, $f'(\xi,\eta)$ decreases initially to about $\eta \approx 2.7$, after which a cross-over occurs, i.e. as one moves out towards the edge of the boundary layer as shown in Fig. 8. Namely, for example, the profile for $\theta_r = 1.1$ is higher than that of $\theta_r = 1.6$ up to $\eta \approx 2.7$ after which the converse is apparent, i. e., θ_r causes higher velocities toward the edge of the boundary layer. The results presented demonstrate quite clearly that the variation of viscosity with temperature has a substantial effect on the flow and heat transfer characteristics. Further, the results in Table 4 indicate that the wall shear stress $f''(\xi,0)$ and the local Nusselt number $Nu_x Re_x^{-1/2}$ decrease as the viscosity-temperature parameter θ_r increases.

Figures 10 and 11 present the behavior of the velocity $f'(\xi,\eta)$ and temperature $\theta(\xi,\eta)$ profiles for the VWT case for various values the thermal conductivity parameter δ. As δ increases, i. e. the thermal conductivity increase with temperature, both velocity and temperature in the respective boundary layers increase. This can be attributed to the fact that increasing the thermal conductivity parameter increases the fluid thermal conductivity which, in turn, increases its temperature and velocity. Moreover, the rise in the magnitude of velocity and temperature is quite significant in the present case, showing that the volume rate of flow at a section perpendicular to the sheet increases with the increase in the δ values. Also, the results presented demonstrate quite clearly that the variation of thermal conductivity with temperature has a substantial effect on the flow and heat transfer characteristics. In addition, from Table 4 it is seen that the wall shear stress $f''(\xi,0)$ and the local Nusselt number $Nu_x Re_x^{-1/2}$ are greatly increased as the thermal conductivity parameter δ increases.

Figures 12 and 13 present typical velocity $f'(\xi,\eta)$ and temperature $\theta(\xi,\eta)$ profiles in the boundary layer adjacent to the surface for various values of the buoyancy force parameter ξ for the VWT case, respectively. Increases in the values of ξ have the tendency to induce more flow in the boundary layer due to the effect of the thermal buoyancy. For small buoyancy effects ($\xi \leq 2$), the maximum flow velocity occurs at the surface. However, as the buoyancy effects get relatively large, a distinctive peak in the velocity profile occurs in the fluid adjacent to the wall and this peak becomes more distinctive as ξ increases further. Along with this flow behavior, the thermal boundary layer reduces as ξ increases causing the fluid temperature to reduce at every point other than that of the wall. These flow and thermal behaviors are depicted by the respective increases and decreases in the velocity and temperature fields as ξ increases shown in Figs. 12 and 13. Moreover, the numerical results in Table 4 show that the wall shear stress $f''(\xi,0)$ and the local Nusselt number $Nu_x Re_x^{-1/2}$ are both increased with increasing ξ. This is due to the fact that positive ξ induces a favorable pressure gradient that enhances the fluid flow and heat transfer in the boundary layer. Figures 14 and 15 illustrate the changes that are brought about in the velocity and temperature profiles due to changes in the values of spatial-dependent internal heat generation ($A^* > 0$) or absorption ($A^* < 0$) in the boundary layer flow region for the VWT case, respectively. The presence of a heat source ($A^* > 0$) in the boundary layer generates energy which causes the temperature of the fluid to increase. This increase in temperature has a direct effect in increasing the thermal buoyancy forces which, in turn, increases the velocity of the flow. On the other hand, the presence of a heat sink ($A^* < 0$) in the boundary layer absorbs energy which causes the temperature of the fluid

to decrease. This decrease in the fluid temperature causes a reduction in the flow velocity in the boundary layer as a result of the buoyancy effect which couples the flow and thermal problems. These behaviors are depicted in Figs. 14 and 15. Further, from Table 4 we notice that the local Nusselt number $Nu_x Re_x^{-1/2}$ decreases whereas the wall shear stress $f''(\xi,0)$ increases as A^* increases.

The influence of the temperature-dependent internal heat generation ($B^* > 0$) or absorption ($B^* < 0$) in the boundary layer on the flow and thermal fields for the VWT case is the same as that of spatial-dependent internal heat generation or absorption but with significant effect. Namely, for $B^* > 0$ (heat source), the velocity and temperature of the fluid increase while they decrease for $B^* < 0$ (heat sink). These behaviors are depicted in Figs. 16 and 17. Also, the local Nusselt number $Nu_x Re_x^{-1/2}$ decreases while the wall shear stress $f''(\xi,0)$ increases due to an increase in the temperature-dependent internal heat generation/absorption B^*. In addition, the value of $B^* = 1$ represent a large value of a heat source that causes the temperature of the fluid near the sheet to be higher than the wall temperature as shown in Fig. 17. Consequently, the wall heat transfer is reversed. Also, the local Nusselt number $Nu_x Re_x^{-1/2}$ decreases while the wall shear stress $f''(\xi,0)$ increases due to an increase in the value of B^* as shown in Table 4. It is noted that the negative heat transfer rates are obtained for higher values of B^* (e.g., $B^* = 1$ and 1.5). Negative values of $Nu_x Re_x^{-1/2}$ indicate that heat is transferred from the fluid to the moving surface as discussed before. Figures 2-17 are also the graphical representation of the velocity $F'(\zeta,\eta)$ and temperature $\phi(\zeta,\eta)$ profiles in VHF case for the same physical parameters used in VHF case. Effects of all physical parameters on the flow and thermal fields are noticed to be qualitatively similar but with quantitatively increased magnitude (except for the effect of velocity slip parameter λ on the velocity profiles as shown in Fig. 2), especially the temperature, as compared to the VWT case. Comparison study of the velocity profiles for both VWT and VHF cases reveals that the velocity profiles for the VHF case are higher than those of the VWT case as shown in Figs. 2, 4, 6, 8, 10, 12, 14 and 16. In other words, the VHF boundary condition induces more flow in the boundary layer region than that of the VWT boundary condition. Also, on comparing the temperature distribution of the VWT and VHF cases it is apparent that the VHF boundary condition succeeds in keeping the cooling liquid warmer than in the case when VWT boundary condition is applied. It may therefore be inferred that the VWT boundary condition is better suited for faster cooling of the stretching sheet than the variable heat flux boundary condition case. From Figs. 6, 10, 12, 14 and 16 it is clear that, in the VHF case, there exist an overshooting of the velocity over the moving speed of the sheet for small values of R (e.g., $R = 0.2, 0.6$) and higher values of δ and ε (e.g., $\delta = \varepsilon = 2, 3$), A^*(e.g., $A^* = 1, 1.5$), B^* (e.g. $B^* = 1$) and the buoyancy force parameters (ξ and ζ). Also, the difference in magnitude of the velocity in both VWT and VHF cases is more apparent for lower R values than for higher R values, as indicated by the greater separation of curves for $R = 0.2, 0.6$ than when $R = 5$ as shown in Fig. 6. The opposite result was observed on the behavior of the velocity for both VWT and VHF cases as θ_r, ϕ_r , δ, ε, A^*, B^* and the buoyancy force parameters (ξ and ζ) increase as shown in Figs. 8, 10, 12, 14 and 16. From Figs. 3, 5, 7, 9, 11, 13, 15 and 17 it is noticed, by comparison study of the temperature profiles for both VWT and VHF cases, that wall temperature would be significantly higher in VHF case as compared to the VWT case. This is owing to the fact that in VHF case thermal boundary layer thickness is higher.

Values of $F''(\zeta,0)$ and $Nu_x Re_x^{-1/2}$ in the VHF case for the same physical parameters presented in Table 4 are listed in Table 5. Effects of all physical parameters on the wall shear stress $F''(\zeta,0)$ and the local Nusselt number $Nu_x Re_x^{-1/2}$ are noticed to be similar as compared to the VWT except that the local Nusselt number $Nu_x Re_x^{-1/2}$ decreases with increasing the thermal conductivity parameter χ. Comparison study of Tables 4 and 5 indicates that the wall shear stress $F''(\zeta,0)$ for the VHF case is higher than that of the VWT case for all values of λ, M, R, θ_r, ϕ_r, δ, ε, A^*, B^* and the buoyancy force parameter ζ. In Tables 4 and 5 we have extracted information for both the VWT and VHF cases on the local Nusselt number $Nu_x Re_x^{-1/2}$. Clearly, the local Nusselt number $Nu_x Re_x^{-1/2}$ for the VWT case is higher than that of the VHF case for all values of the slip param-

eter, magnetic field parameter, variable viscosity parameters (θ_r and ϕ_r) and the buoyancy force parameters (ξ and ζ). On the other hand, the local Nusselt number $Nu_x Re_x^{-1/2}$ for the VWT case is lower than that of the VHF case for lower values of the radiation parameter ($0 < R \leq 0.8$), while the opposite result was observed for higher values of it ($R > 0.8$). Finally, the numerical results in Tables 4 and 5 show that the local Nusselt number $Nu_x Re_x^{-1/2}$ for the VWT case is higher than that of the VHF case for a heat sink ($A^* < 0$ and $B^* < 0$) and the opposite behavior is seen for a heat source ($A^* > 0$ and $B^* > 0$).

4 Conclusion

The effects of radiation, temperature dependent viscosity and thermal conductivity, on the MHD mixed convection slip flow and heat transfer from a heated stretching surface in the presence of a transverse magnetic field, heat generation/absorption have been studied. An analysis has been carried out to investigate the thermal transport phenomenon for two general thermal boundary conditions, namely (I) variable wall temperature (VWT) and (II) variable surface heat flux (VHF) of the power-law form. The governing equations were developed and transformed using appropriate non-similarity variables and solved numerically. The specific conclusions derived from this study can be listed as follows:

1. The velocity and temperature profiles depend strongly on the nature of the boundary conditions on the velocity and temperature (i.e., whether wall temperature or heat flux is variable at the wall).

2. The wall temperature is greatly higher in the VHF case as compared to the VWT case for all values of the slip parameterλ, magnetic parameter M, radiation parameter R, viscosity-temperature parameter θ_r, thermal conductivity parameter ε, space-dependent internal heat generation/absorption A^*, temperature-dependent internal heat generation/absorption B^* and buoyancy force parameter ζ and hence the VWT boundary condition is better suited for effective cooling of the stretching sheet.

3. The velocity in the boundary layer region is higher in the VHF case as compared to the VWT case for all values of M, ϕ_r, ε, R, A^*, B^* and the buoyancy force parameter ζ and this rise in the value of the velocity is more significant for lower values of R and higher values of all other parameters.

4. The wall shear stress decreases with increasing the parameters of magnetic field, radiation and the viscosity-temperature, but it increases with increasing the slip parameter, thermal conductivity, space-dependent and temperature-dependent internal heat generation/absorption and buoyancy force parameters in both the VWT and VHF cases.

5. The local Nusselt number decreases with an increase in the values of slip parameter, magnetic field, viscosity-temperature and space-dependent and temperature-dependent internal heat generation /absorption parameters, whereas it increases with increasing the radiation and buoyancy force parameters in both the VWT and VHF cases.

6. Increasing the thermal conductivity parameter was found to cause reductions in the values of local Nusselt number in the VHF case, but the reverse trend was observed in the VWT case as the thermal conductivity parameter increases.

References

[1] E. M. Abo-Eldahab, M. Abd El Aziz, *Hall and ion-slip effects on MHD free convective heat generating flow past a semi-infinite vertical flat plate*, Physica Scripta 61 (2000) 344-348.

[2] E. M. Abo-Eldahab, M. Abd El Aziz, *Hall current and Ohmic heating effects on mixed convection boundary layer flow of a 349 micropolar fluid from a rotating cone with power-law variation in surface temperature*, Int. Comm. Heat Mass Transfer 31 (2004) 751.

[3] E. M. Abo-Eldahab, M. Abd El-Aziz, *Viscous dissipation and Joule heating effects on MHD-free convection from a vertical plate with power-law variation in surface temperature in the presence of Hall and ion-slip cur-*

rents, Applied Mathematical Modelling 29 (2005) 579.

[4] E. M. Abo-Eldahab, M. Abd El-Aziz, A. M. Salem, K. K. Jaber, *Hall current effect on MHD mixed convection flow from an inclined continuously stretching surface with blowing/suction and internal heat generation/absorption*, Appl. Math. Modelling 31 (2007) 1829-1846.

[5] E. M. Abo-Eldahab, M. Abd El-Aziz, *Flow and heat transfer in a micropolar fluid past a stretching surface embedded in a non-Darcian porous medium with uniform free stream*, Appl. Math. Comp. 162 (2005) 881-899.

[6] E. M. Abo-Eldahab, M. Abd El-Aziz, *Blowing/suction effect on hydromagnetic heat transfer by mixed convection from an inclined continuously stretching surface with internal heat generation /absorption*, Int. J. Thermal. Sci. 43 (2004) 709-719.

[7] M. Abd El-Aziz, A. M. Salem,*MHD-mixed convection and mass transfer from a vertical stretching sheet with diffusion of chemically reactive species and space or temperature dependent heat source*, Can. J. Phys. 85 (2007) 359-373.

[8] M. Abd El-Aziz, *Thermal radiation effects on magnetohydrodynamic mixed convection flow of a micropolar fluid past a continuously moving semi-infinite plate for high temperature differences*, Acta Mechanica 187 (2006) 113-127.

[9] M. Abd El-Aziz, *Thermal-diffusion and diffusion-thermo effects on combined heat and mass transfer by hydromagnetic three-dimensional free convection over a permeable stretching surface with radiation*, Phys. Letters A 372 (2007) 263-272.

[10] A. Aziz, *Hydrodynamic and thermal slip flow boundary layers over a flat plate with constant heat flux boundary condition, Commun*, Nonlinear Sci. Numer. Simul. 15 (2010) 573-580.

[11] P. Carragher, L. J. Crane, *Heat transfer on a continuous stretching sheet*, Z. Angew. Math. Mech. 62 (1982) 564-565.

[12] A. Chakrabarti, A. S. Gupta, *Hydromagnetic flow and heat transfer over a stretching sheet*, Q. Appl. Math. 37 (1979) 73-78.

[13] C. K. Chen, M. I. Char, *Heat transfer of a continuous stretching surface with suction or blowing*, J. Math. Anal. Appl. 135 (1988) 568-580.

[14] C. H. Chen, *Laminar mixed convection adjacent to vertical continuously stretching sheets, Heat Mass Transfer 33 (1998) 471-476.*

[15] T. C. Chiam, Hydromagnetic flow over a surface stretching with a power-law velocity, Int. J. Engrg. Sci. 33 (1995) 429-435.

[16] T. C. Chiam, *Heat transfer with variable conductivity in a stagnation-point flow towards a stretching sheet*, Int. Comm. Heat Mass Transfer 23 (1996)239-248.

[17] L. J. Crane, *Flow past a stretching plate*, Z. Angew. Math. Phys. 21 (1970) 645-647.

[18] B. S. Dandapat, S.N. Singh, R.P. Singh,*Heat transfer due to permeable stretching wall in presence of transverse magnetic field*, Arch. Mech. 56 (2004) 87-101.

[19] N. Datta, B. Mazumder, *Hall effects on hydrodynamic free convection flow past an infinite porous flat plate*, J. Math. Phys. Sci. 10 (1975) 59.

[20] B. K. Dutta, P. Roy, A. S. Gupta,*Temperature field in flow over a stretching sheet with uniform heat flux*, Int. Comm. Heat Mass Transfer 12 (1985) 89-94.

[21] E. M. A. Elbashbeshy, M. A. A. Bazid, *Heat transfer over an unsteady stretching surface*, Heat Mass Transfer 41 (2004) 1-4.

[22] R. S. R. Gorla, J. Lee, S. Nakamura, I. Pop, *Effects of transverse magnetic field on mixed convection in wall plume of power law fluids*, Int. J. Eng. Sci. 31 (1993) 1035-1045.

[23] L. J. Grubka, K. M. Bobba, *Heat transfer characteristics of a continuous stretching surface with variable temperature*, ASME J. Heat Transfer 107 (1985) 248-250.

[24] P. S. Gupta, A. S. Gupta, *Heat and mass transfer on a stretching sheet with suction or blowing*, Can. J. Chem. Eng. 55 (1977) 744-746.

[25] A. S. Gupta, *Hydrodynamic flow past a porous flat plate with Hall effects*, Acta Mechanica 22 (1975) 281.

[26] D. R. Jeng, T. C. A. Chang, K. J. DeWitt, *Momentum and heat transfer on a continuous moving surface*, ASME J. Heat Transfer 108 (1986) 532-539.

[27] M. Katagiri, *The effect Hall currents on the viscous flow magnetohydrodynamic boundary layer flow past a semi-infinite flat plate*, J. Phys. Soc. Japan 27 (1969) 1051.

[28] M. Kumari, H. S. Takhar, G. Nath, *MHD flow and heat transfer over a stretching surface with prescribed wall temperature or heat flux*, Wärme- und Stoffübertragung 25 (1990) 331-336.

[29] J. X. Ling, A. Dybbs, ASME, *Paper 87-WA/HT-23, ASME winter annual meeting, Boston*, Massachusetts 13-18 (1987).

[30] S. J. Liao, *An analytic solution of unsteady boundary-layer flows caused by an impulsively stretching plate*, Comm. in Nonlinear Science and Num. Simulation 11 (2006) 326-339.

[31] M. A. A. Mahmoud, *Thermal radiation effects on MHD flow of a micropolar fluid over a stretching surface with variable thermal conductivity*, Physica A 375 (2007) 401-410.

[32] A. Moutsoglou, T. S. Chen, *Buoyancy effects in boundary layers on inclined*, continuous moving sheets ASME J. Heat Transfer 102 (1980) 371-373.

[33] S. Mukhopadhyay, *Effects of slip on unsteady mixed convective flow and heat transfer past a porous stretching surface*, Nuclear Eng. Design 241 (2011) 2660-2665.

[34] T. Y. Na, I. Pop, *Unsteady flow past a stretching sheet*, Mech. Res. Comm. 23 (1996) 413-422.

[35] T. Y. Na, *Computational Methods in Engineering Boundary Value Problems*, Academic Press, New York (1979).

[36] R. Nazar, N. Amin, D. Filip, I. Pop, *Unsteady boundary layer flow in the region of the stagnation point on the stretching sheet*, Int. J. Eng. Sci. 42 (2004) 1241-1253.

[37] I. Pop, V. M. Soundalgekar, *Effects of Hall current on hydromagnetic flow near a porous plate*, Acta Mechanica 20 (1974) 315-318.

[38] I. Pop, T. Watanabe, *Hall effect on magnetohydrodynamic free convection about a semi-infinite vertical flat plate*, Int. J. Eng. Sci. 32 (1994) 1903.

[39] T. A. Savvas, N. C. Markatos, C. D. Papaspyrides, *On the flow of non-Newtonian polymer solutions*, Appl. Math. Model. 18 (1994) 14-22.

[40] B. Sahoo, Flow and heat transfer of a non-Newtonian fluid past a stretching sheet with partial slip, Commun. Nonlinear Sci. Numer. Simul. 15 (2010) 602-615.

[41] H. Sato, *The Hall effect in the viscous flow of ionized gas between two parallel plates under transverse magnetic field*, J. Phys. Soc. Japan 16 (1961) 1427.

[42] A. M. Salem, M. Abd El-Aziz, *Effect of Hall currents and chemical reaction on hydromagnetic flow of a stretching vertical surface with internal heat generation/absorption*, Appl. Math. Modelling 32 (7) (2008) 1236-1254.

[43] H. Schilichting, *Boundary Layer Theory, McGraw-Hill*, New York, pp 266, 1972.

[44] G. W. Sutton, A. Sherman, *Engineering Magnetohydrodynamics, McGraw-Hill*, New York, 1965.

[45] Y. Tan, S. J. Liao, *Series solution of three-dimensional unsteady laminar viscous flow due to a stretching surface in a rotating fluid*, ASME J. Appl. Mech. 74 (2007) 1011-1018.

[46] I. Tani, *Steady motion of conducting fluids in channels under transverse magnetic fields with consideration of Hall effect*, J. Aerospace Sci. 29 (1962) 287.

[47] J. Vleggaar, *Laminar boundary-layer behaviour on continuous, accelerating surfaces*, Chem. Eng. Sci. 32 (1977) 1517-1525.

[48] C. Y. Wang , G. Du, M. Miklavi, C. C. Chang, *Impulsive stretching of a surface in a viscous fluid*, SIAM J. Appl. Math. 57 (1997) 1-14.

[49] M. R. Warren, P. H. James, I. C. Young, *Handbook of heat transfer*, 3rd ed. Chap. 7, McGraw-Hill, USA, pp. 21-23 (1998).

[50] R. C. Weast, *Hand book of chemistry and physics, 67th ed. Boca Raton*, Fl: C.R.C. Press pp. 1986-1987

[51] H. Xu, S. J. Liao, I. Pop, *Series solutions of unsteady three-dimensional MHD flow and heat transfer in the boundary layer over an impulsively stretching plate*, Eur. J. Mech. B/Fluids 26 (2007) 15-27.

[52] T. Yamanishi, *Hall effect in the viscous flow of ionized gas through straight channels*, in: 17th Annual Meeting, Phys. Soc. Japan 5 (1962) 29.

Mohamed Abd El-Aziz was born in Egypt, in March, 1972. He completed Master of Science, degree in Mathematics (1999) from Helwan University, and is pursuing PhD in Fluid Dynamics, Helwan University. He worked as lecturer in the Department of Mathematics, College of Science, Helwan University, Egypt, for five years (1999-2004). He was the Assistant Professor in the Department of Mathematics, College of Science, Helwan University, Egypt From September 2004 to August 2007, and in College of Science, KKU university, Abha, Saudi Arabia from August 2004 to July 2011. From July 2011 to till date he is working as Associate Professor in the Department of Mathematics, College of Science, KKU University, Abha, Saudi Arabia. He guided 1 PhD, 4M. Sc. and has published more than 25 Research papers in National and International Journals.